26th EPS Conf. on Contr. Fusion and Plasma Physics, Maastricht, 14 - 18 June 1999 ECA Vol.23J (1999) 1469 - 1472

ECRH Absorption and Shafranov Shift in the "Electron Root" Feature at the W7-AS Stellarator

Ch. Fuchs, J. Geiger, H.J. Hartfuß, H. Maaßberg, and the W7-AS Team

Max-Planck-Institut für Plasmaphysik, EURATOM Ass., D-85748 Garching, Germany

Introduction

The "electron root" feature with the centrally peaked electron temperature profiles ($T_i \ll T_e \leq 6\,\mathrm{keV}$) is observed in low density ECRH discharges at sufficient power level (up to 1.3 MW at 140 GHz $2nd$ harmonic X-mode for $B \simeq 2.5\,\mathrm{T}$). A strongly positive radial electric field E_r in the central region reduces the neoclassical electron heat diffusivity and allows for the very steep T_e gradients [1].

The highly peaked pressure profile obtained under these conditions, $\beta(r)$, leads to a significant Shafranov shift in the central region. Furthermore, the bootstrap current at outer radii is compensated by an induced ohmic one which peaks in the center for the typical zero net current W7-AS operation. For these conditions, the central rotational transform ι is strongly reduced leading to an increased (outward) Shafranov shift. On the other hand, a significant amount of the ECRH power must be deposited close to the magnetic axis in order to drive the "electron root" feature. For increased temperature, however, the wave absorption is shifted inward due to the relativistic resonance condition $\omega - k_\parallel v_\parallel - l\omega_{ce}(B)/\gamma = 0$ (with γ being the relativistic factor). These two effects are supposed to be the cause of the observed phenomenon of irregular or sometimes harmonic switching between the ion root and the electron root regime (figure 1). The change of the temperature profile leads to a change of the Shafranov shift d_s which has to be properly considered when interpreting the ECE spectrum in terms of a temperature profile. An example is given in figure 2. The temperature changes $\Delta T_e(r)$ in the inner region (channels 1 to 3) dominate over the term $d\,T_e/d\,r \cdot \Delta d_s$ of the Shafranov shift. For channel 4 the equation $d\,T_e/d\,r \cdot \Delta d_s - \Delta T_e \simeq 0$ is satisfied, leading to a compensation of the effects. For channels 5 and 6 with small $\Delta T_e(r)$, the signal changes are domiated by the Shafranov shift. The phases of the low field (6) and the high field side (5) channels are opposite as expected.

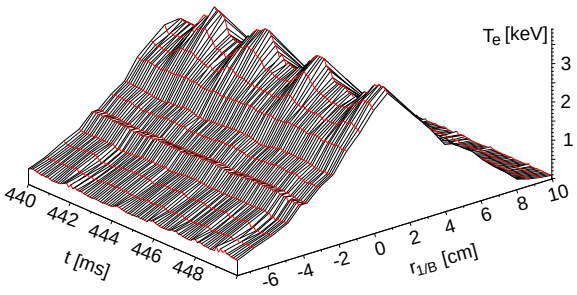

Fig. 1. *Oscillations between the ion and the electron root regime, measured by 24 ECE channels.*

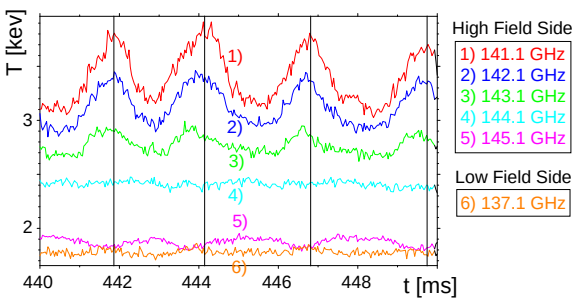

Fig. 2. *Selection of five high field side channels and one low field side channel.*

The centrally peaked T_e profile vanishes within about 1 ms after the ECRH power is switched below the threshold level. Numerical calculations of the temporal evolution of the temperature profile (see below) lead to a qualitative agreement with temperature signals of the central ECE channels. For a more detailed comparison between calculations and experimental data, the frequencies of the ECE-channels have to be assigned to the correct B profile. One possibility to accomplish this is to try to interpolate between equilibrium calculations (VEMEC code). The other possibility is to perform approximate (fast) calculations of the Shafranov shift d_s.

Calculation of the Shafranov shift and the B-field along the ECE sightline

The Shafranov shift $d_s(r)$ is defined as the absolute outward shift of the flux surface with effective radius r. It is caused by the pressure driven Pfirsch-Schlüter (PS) currents which can be calculated by solving the equation

$$\nabla(\mathbf{j}^{PS} + \mathbf{j}^{dia}) = 0$$

with $\mathbf{j}^{dia} = \nabla\mathbf{p} \times \mathbf{B}/B^2$ being the diamagnetic current density. For a large aspect ratio machine, an approximate solution in cylindrical geometry is

$$\mathbf{j}^{PS} = -\frac{2\,p\prime\,\beta^*_{10}}{B_0\,\iota}\,\cos\theta \qquad \text{with} \quad p\prime = \frac{\partial p}{\partial r}.$$

B_0 is the flux density on plasma axis, θ the poloidal angle and β^*_{10} the averaged toroidal curvature, translating an elongated into a cylindrical geometry and being 0.7 for W7-AS. The vector potential from the mainly parallel PS currents can be written in the form $A^{PS}_\varphi(r)\,\mathbf{e}_\varphi\,\cos\theta$. Integration of the PS currents leads to

$$A^{PS}_\varphi(r) = -\frac{2\,\mu_0\,\beta^*_{10}}{B_0}\frac{1}{r}\int_0^r y \int_a^y \frac{p\prime(x)}{\iota(x)}\,dx\,dy\,.$$

This vector potential adds to the vector potential $A^{\iota}_\varphi(r)$ caused by the external ι part and by toroidal currents which give rise to a radial variation of the otherwise flat ι profile. The equation

$$A^{\iota}_\varphi(r) = \frac{B_0}{\beta^*_{10}\,R}\int_0^r x\,\iota(x)\,dx$$

with R being the major radius can easily be derived.
A flux surface is defined by $A_\varphi(r,\theta) = A^{\iota}_\varphi(r) + A^{PS}_\varphi(r)\,\cos\theta = const.$ To find the Shafranov shift $d_S(r)$ for each flux surface, the following method is applied. For the vector potential A_φ, only $\theta = 0$ and $\theta = \pi$ is considered. In this way, $A(r)$ can be calculated (figure 3):

$$\begin{aligned} A(r) &= A^{\iota}_\varphi(-r) - A^{PS}_\varphi(-r) \quad \text{for } r < 0 \\ A(r) &= A^{\iota}_\varphi(r) + A^{PS}_\varphi(r) \quad \text{for } r \geq 0\,. \end{aligned}$$

The negative r values are assigned to the high field side where $\theta = \pi$. The position of the minimum is the central shift $d_S(0)$. Stepping numerically to lower radii from $d_S(0)$

to position r_1 and finding r_2 where $A_\varphi(r_2) = A_\varphi(r_1)$, the Shafranov shift can be obtained for every r: $r = 1/2(r_2 - r_1)$ and $d_s(r) = 1/2(r_1 + r_2)$. The $d_s(r)$ function is then used to derive the B-field of the horizontal ECE sightline (which is slightly above the plasma axis) from the vacuum field. At last, the B-field is corrected for the diamagnetic effect by multiplying $B(r)$ by $\sqrt{1-\beta}$ with $\beta = 2\,\mu_0\,p/B^2$. A comparison of the resulting $B(r)$ function with VEMEC calculations is shown in figure 4. Although W7-AS is far from axisymmetry, a good agreement between these calculations is obtained. This can be explained by mainly undisturbed parallel PS currents around the torus without significant current curls. Using $B(r)$, the electron temperature T_e and the effective radius r can easily be derived for all ECE channels. The numerical calculation is fast, opening the possibility to model temporal changes of the T_e profile with respect to measured signals in ECE. This is demonstrated in the next section.

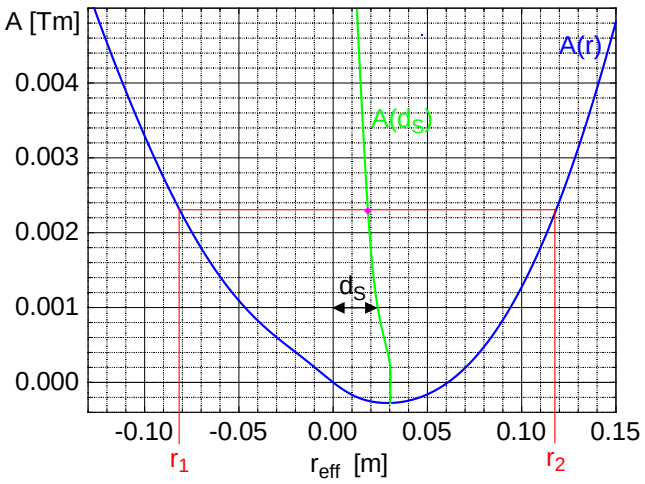

Fig. 3. *Vector potential A for assumed ι and p profiles.*

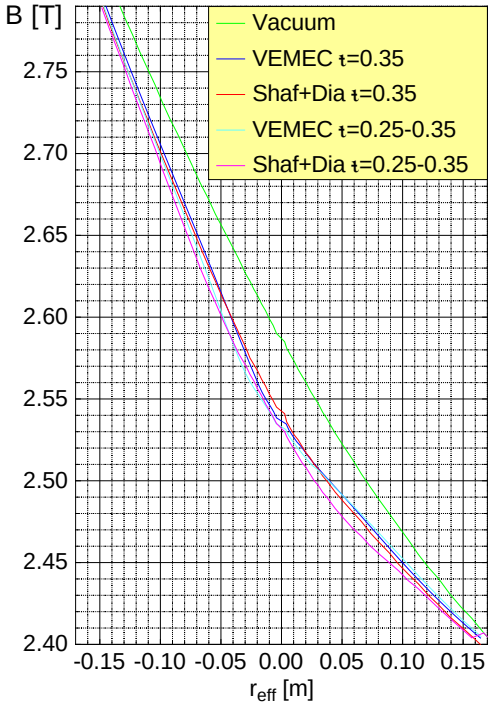

Fig. 4. *Comparison between the B field mapping as calculated with the VEMEC code and the Shafranov shift.*

Comparison between calculated and measured time traces of ECE channels

A temperature profile is calculated using a neoclassical electron root model for $\chi(E_r)$. The radial extent and the magnitude of the strongly positive electric field are chosen to match the central T_e profile of a plasma discharge in the electron root regime before the ECRH power of 750 kW is switched off (see figure 5). The E_r field in the electron root model vanishes exponentially with a time constant of 0.6 ms (see figure 6), leading to a fast decline of the central temperature. The calculated T_e profiles, adjusted density profiles (to get the proper pressure profile) and estimated current profiles are used for a calculation of the Shafranov shift $d_S(r,t)$ and the radial locations $r(t)$ of the radiation measured by the ECE system (see figure 7). The temperature $T_e(t)$ is also computed and compared with the experimental data, which is shown in figure 8. The high electric conductivity of the plasma leads to time constants for the current diffusion in the central region of the order of 1 s so that the initial current profile (and accordingly the ι profile) is assumed to be constant in the considered time frame.

Conclusion

Even for a three dimensional topology of flux surfaces it is possible to obtain sufficently exact results for the Shafranov shift with fast calculations. These can be used to calculate the B field along the ECE sightline. In this way it is possible to model the time tracks of the ECE signals for a study of the switching behavior in the electron root regime. Presently only a few ECE channels lie in the central region of the plasma. An additional ECE system with high spatial resolution will be installed at W7-AS in near future, allowing far more detailed investigations.

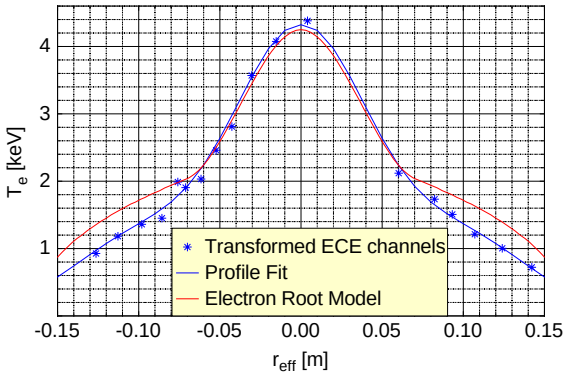

Fig. 5. *The measured T_e profile is transformed using a VEMEC equilibrium. The parameters for the electron root model were chosen accordingly.*

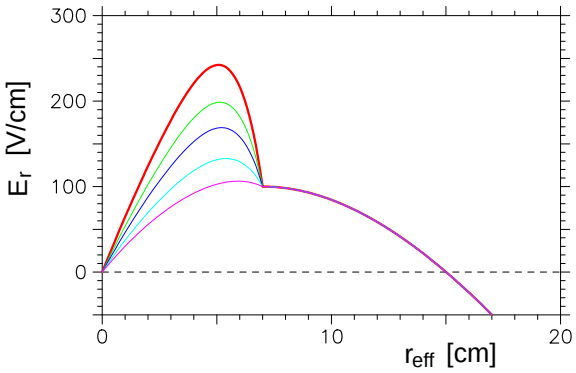

Fig. 6. *Temporal evolution of the E_r profile. The times for which the profiles are plotted are 0, 0.2, 0.4, 0.8 and 1.6 ms.*

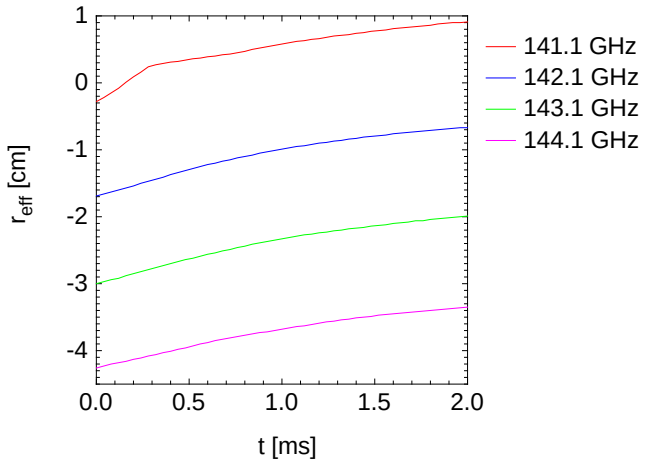

Fig. 7. *Calculated positions where the radiation at fixed frequencies comes from.*

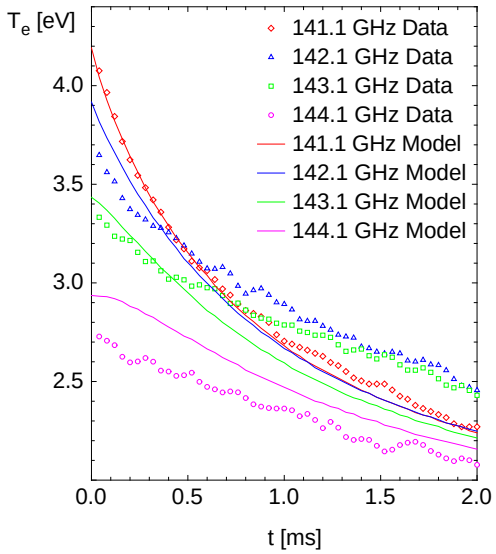

Fig. 8. *Comparison between measured and calculated ECE signals.*

References

[1] M Kick, H Maaßberg, M Anton, J Baldzuhn, M Endler, C Görner, M Hirsch, A Weller, S Zoletnik and the W7-AS Team, Plasma Phys. Control. Fusion **41**, A549 (1999).